= 52.6 kcal mol^{-1}, in fair agreement with this work. Finally, the similarity of the kinetic parameters reported here to those for the decomposition of other four-membered rings,[18] the thermal stability of **7** under these conditions, and the kinetics of the silene isomerization mitigate against the suggestion of a multistep diradical mechanism for the formation of **2** from **3**.

Acknowledgment. We gratefully acknowledge the financial support of the Robert A. Welch Foundation and the N.T.S.U. Faculty Research Fund. We thank Professor H. M. Frey for a stimulating introduction to the methods of gas-phase kinetics and Professor W. R. Dolbier, Jr., for advice on the construction of a salt bath.

Registry No. 1, 38062-40-0; **2**, 6376-86-9; **3**, 765-33-3; **4**, 55544-25-7; **5**, 18187-50-3; **6**, 16054-12-9; **7**, 89530-22-3; C_2H_4, 74-85-1; C_3H_6, 115-07-1; butadiene, 106-99-0.

(18) Robinson, P. J.; Holbrook, K. A. "Unimolecular Reactions"; Wiley: New York, 1972; pp 193-196.

Spectroscopic Studies on Ferrous Non-Heme Iron Active Sites: Variable-Temperature MCD Probe of Ground- and Excited-State Splittings in Iron Superoxide Dismutase and Lipoxygenase

James W. Whittaker and Edward I. Solomon*

Department of Chemistry, Stanford University
Stanford, California 94305
Received June 21, 1985

The ferrous non-heme iron active sites in iron superoxide dismutase (FeSD) and soybean lipoxygenase (SBL) catalyze, respectively, superoxide dismutation[1] and lipid hydroperoxidation.[2] Structures are lacking for the ferrous sites in these proteins, and while the ferric active sites have been characterized by optical and EPR spectroscopy,[3,4] comparable results are lacking for the ferrous sites. MCD spectroscopy is a powerful probe of these systems in that selection rules allow the observation of weak d-d transitions, and the temperature dependence probes ground-state splittings.[5] Using low-temperature MCD spectroscopy we have observed significant differences in both ground and excited states of the iron sites in FeSD and SBL which relate to differences in coordination number and geometry.

FeSD and SBL were purified to homogeneity (SDS-PAGE) from *E. coli* cell paste[3] and soybeans[6] according to published procedures. The low-temperature (1.8 K), high-field (6 T) MCD spectrometer will be described elsewhere.[7]

A distinction between FeSD and SBL iron sites is evident in the excited-state spectra shown in Figure 1: near-IR optical absorption, CD, and low-temperature MCD spectra for FeSD (Figure 1A) show a single broad transition above 10000 cm^{-1} with a low extinction coefficient (ϵ = 5 M^{-1} cm^{-1}) characteristic of ligand field transitions; a second band is observed in absorption near 5000 cm^{-1}. In contrast, the near-IR CD and MCD for SBL (Figure 1B) resolve two broad bands near 10000 cm^{-1} split by approximately 1500 cm^{-1}.

The temperature-dependent MCD of these ligand-field transitions probes the iron ground states in these two enzymes. Systematic variations of temperature and field strength lead to changes in MCD intensity which may be plotted as saturation magnetization curves,[8,9] shown in the Figure 2A for the FeSD

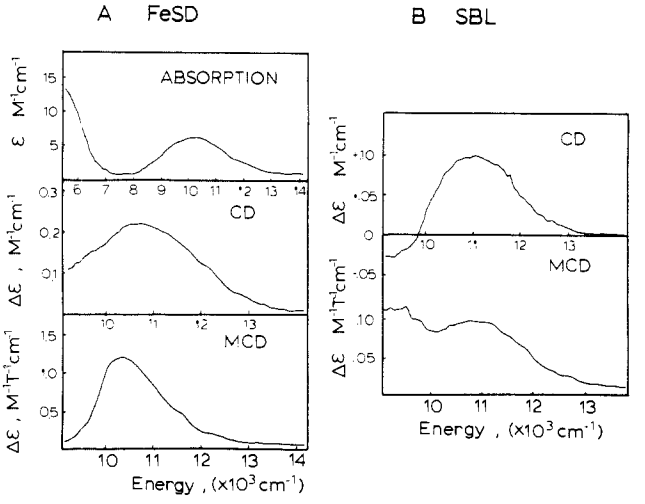

Figure 1. Excited-state spectra for non-heme iron active sites of FeSD and SBL. (A) Optical absorption, CD, and low-temperature MCD spectra for Fe^{2+} SD prepared by dithionite reduction of native enzyme in 50 mM K_2HPO_4 buffer pH 7.4. Note abscissa scale change for optical absorption spectrum. For optical absorption measurements, FeSD was lyophilized and dissolved in D_2O; the MCD sample was prepared as a glass in 50% glycerol. Samples were 3-7 mM Fe; MCD spectrum recorded at 4.2 K in a 3-mm path length cell. (B) CD and MCD spectra for native ferrous SBL in 50 mM sodium borate pH 9.0; the MCD sample was prepared as a glass in 50% glycerol. Samples were 1-2 mM Fe; MCD spectrum recorded at 4.2 K in a 3-mm path length cell. Efforts to observe these bands in absorption are complicated by turbidity at high protein concentration; we can only place an upper limit on ϵ of 5 M^{-1} cm^{-1}.

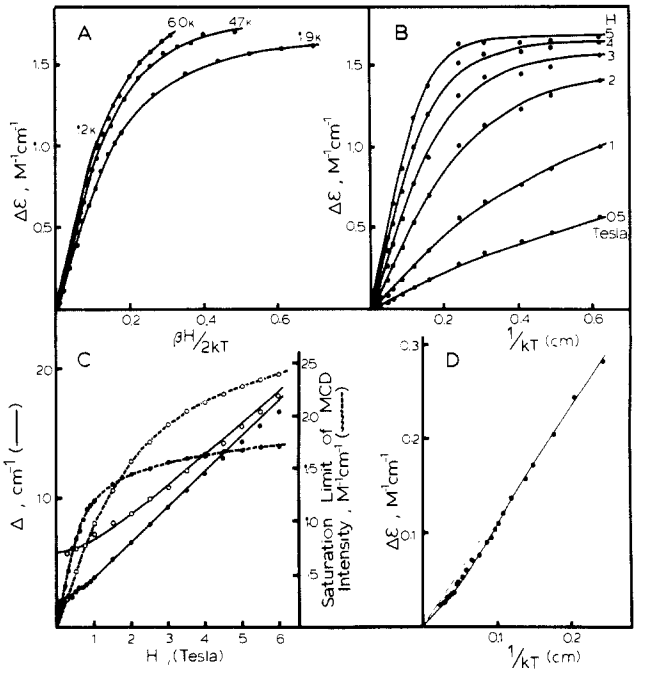

Figure 2. Temperature and field dependence of MCD intensity. (A) Saturation magnetization curves for Fe^{2+} SD for MCD intensity at 10360 cm^{-1}. Similar results are observed for SBL. (B) Replot of data in (A) as temperature dependence at constant field. (C) Splitting Δ (—) and intensity (---) for the ground $M_s = \pm 2$ doublet extracted from the curves of (B), (●) FeSD. Also shown for SBL (○).

data. Magnetic saturation occurs within a paramagnetic ground state when thermally accessible levels are depopulated from either high-field splitting or low temperature. For zero-field split systems and in particular the non-Kramers (even electron) systems in-

(1) Yost, F. J., Jr.; Fridovich, I. *J. Biol. Chem.* **1973**, 4905-4908.
(2) Theorell, H.; Holman, R. J.; Akeson, A. *Acta Chem. Scand.* **1947**, *1*, 571.
(3) Slykehouse, T. O.; Fee, J. A. *J. Biol. Chem.* **1976**, *251*, 5472-5477.
(4) de Groot, J. J. M. C.; Garssen, G. J.; Veldink, G. A.; Vliegenthart, J. F. G.; Boldingh, J. *FEBS Lett.* **1975**, *56*, 50-54.
(5) Stephens, P. J. *Adv. Chem. Phys.* **1976**, *35*, 197-264.
(6) Finazzi-Agro, A.; Avigliano, L.; Veldink, G. A.; Vliegenthart, J. F. G.; Boldingh, J. *Biochem. Biophys. Acta* **1973**, *326*, 462-470.
(7) Spira, D. J.; Allendorf, M. D.; Solomon, E. I., (unpublished results).
(8) Thomson, A. J.; Johnson, M. K. *Biochem. J.* **1980**, *191*, 411-420.
(9) Schatz, P. N.; Mowery, R. L.; Krausz, E. R. *Mol. Phys.* **1978**, *35*, 1537-1557.

0002-7863/86/1508-0835$01.50/0

vestigated here, changes in MCD intensity resulting from population of higher levels leads to nesting of saturation magnetization curves taken at different temperatures[10] as shown in Figure 2A for the FeSD data. Alternatively, plotting the temperature dependence at constant field separates the temperature and field effects (Figure 2B) and shows that in the saturation limit the MCD intensity is field-dependent, unlike the field-independent behavior observed for a Kramers doublet.

Analysis of these curves (Figure 2B) provides insight into the nature of the ground-state splittings in these complexes in terms of an $S = 2$ spin Hamiltonian with parameters D and E, the axial and rhombic zero-field splitting components. The MCD temperature dependence at each field is consistent with thermal population over a pair of levels with no contribution from higher levels, indicating $D < 0$ which places $M_s = \pm 2$ lowest. Alternative schemes including $D > 0$ are not consistent with the observed data or with parallel studies on model complexes.[11] Both the $M_s \pm 2$ doublet splitting Δ due to rhombic splitting plus the Zeeman interaction and the MCD saturation limit intensity can be obtained by fitting each of the curves in Figure 2B by a Boltzmann population over these two levels.[12] The changes in Δ and saturation limit intensity for increasing field for both FeSD and SBL are plotted in Figure 2C.

An explanation of Figure 2C can be obtained in terms of the appropriate spin Hamiltonian matrix for an isolated $M_s = \pm 2$ doublet:[13]

$$\hat{\mathcal{H}} = \begin{array}{c} \\ |2^s\rangle \\ |2^a\rangle \end{array} \begin{array}{c} \begin{array}{cc} |2^s\rangle & |2^a\rangle \end{array} \\ \begin{bmatrix} +\delta/2 & g\beta H\cos\theta \\ g\beta H\cos\theta & -\delta/2 \end{bmatrix} \end{array} \quad (1)$$

A rhombic zero-field distortion (δ) removes the degeneracy of this non-Kramers doublet, quenching its angular momentum and eliminating MCD intensity. In a magnetic field, the lowest level can be represented as $|-\rangle = C_1|+2\rangle - C_2|-2\rangle$, where the mixing coefficients are $C_2 = ((\delta/g\beta H\cos\theta)^2 + 1)^{-1}$ and $C_1 = (1 - C_2^2)^{1/2}$. The change in energy of the levels with increasing field relates to the Zeeman interaction, while the MCD intensity reflects the complex component of the wavefunctions, which change from pure real combinations in the zero field limit to pure imaginary at high fields. Analysis of Figure 2C in terms of the spin Hamiltonian for the ground doublet (eq 1) with orientation averaging[8,9] yields $g_{eff} = 8$ and $\delta = 2.2$ cm^{-1} for FeSD and $g_{eff} = 8$, $\delta = 6$ cm^{-1} for SBL. In both proteins a doublet is lowest, indicating $D < 0$. The magnitude of D is most directly obtained from the temperature dependence at a small sampling field[14] (0.5 T for FeSD in Figure 2D). The curve is not very sensitive to the value of D but we estimate $D = -7 \pm 2$ cm^{-1}. For SBL no excited-state population is observed but the observed magnitude for $\delta = 3E^2/D$ of 6 cm^{-1} and the fact that E/D must be between 0 and $^1/_3$[15] requires $D > -21$ cm^{-1}.

The ground- and excited-state data on FeSD and SBL is best interpreted in terms of correlations with model complexes. Excited-state splittings and energies over 5- and 6-coordination of Fe^{2+} by N,O and halide ligands is related to geometry,[16] and, in particular, a single band above 10^4 cm^{-1} with a second band at least 3000 cm^{-1} to lower energy implies 5-coordination and approximately square-pyramidal geometry. The presence of two bands near 10000 cm^{-1} with a splitting of 1000 cm^{-1} implies 6-coordination. A supporting correlation can be made from ground-state parameters: $D > 10$ cm^{-1} is representative of 6-coordinate iron, while $D = 2$–10 cm^{-1} is characteristic of 5-coordination.[17] Lower coordination can be ruled out by the energy of the ligand field transitions. From these correlations, we deduce that the most likely coordination number for the SBL ferrous site is six, while the ferrous site in FeSD appears to be 5-coordinate, consistent with the crystallographically determined site structure of Fe^{3+} SD[18,19] being retained upon reduction.

In summary, significant differences have been observed in both excited-state spectra and ground-state spin Hamiltonian parameters as obtained through low-temperature MCD spectroscopy, which indicate differences in coordination environments in these two ferrous non-heme iron active sites.

Acknowledgment. We acknowledge useful discussions with Mark D. Allendorf, Dr. John D. Lipscomb, and Dr. Vincent B. H. Huynh. This investigation was supported by the National Science Foundation (PCM-81-19844) and Public Health Service (1F32-AM07456-01).

Registry No. SBL, 9029-60-1; FeSD, 9054-89-1; Fe, 7439-89-6.

(10) Johnson, M. K.; Robinson, A. E.; Thomson, A. J. In "Iron Sulfur Proteins"; Spiro, T. G., Ed.; Wiley: New York, 1979; pp 367–406.
(11) Whittaker, J. W.; Solomon, E. I., unpublished results.
(12) $A = A_{sat\,limit} \tanh(\Delta/2kT)$
(13) Here, $|2^s\rangle$ and $|2^a\rangle$ are the symmetric and antisymmetric combinations of the pure spin functions diagonal in zero field, δ is the rhombic splitting within the doublet ($3E^2/D$), $g\beta H\cos\theta$ is the orientation-dependent Zeeman interaction for the doublet, and g is the effective g value.
(14) Browett, W. R.; Fucaloro, A. F.; Morgan, T. V.; Stephens, P. J. *J. Am. Chem. Soc.* **1983**, *105*, 1868–1872.
(15) Blumberg, W. E. In "Magnetic Resonance in Biological Systems"; Ehrenberg, A., Malmstrom, B. G., Vänngård, T., Eds.; Pergammon Press: New York, 1983; pp 119–133.
(16) For example, see: (a) Burns, R. G.; Clark, M. G.; Stone, A. J. *Inorg. Chem.* **1966**, *5*, 1268–1272. (b) Gaffney, E. S., *Phys. Rev.* **1973**, *8B*, 3484–3486; (c) Riley, D. P.; Merell, P. H.; Stone, J. A.; Busch, D. H., *Inorg. Chem.* 1975, *14*, 490; (d) Ciampolini, M.; Nardi, N.; Speroni, G. P., *Coord. Chem. Revs.* **1966**, *1*, 222–233; (e) Holmes, O. G.; McClure, D. S., *J. Chem. Phys.* **1957**, *26*, 1686.
(17) For example, see: (a) Hodges, K. O.; Wollmann, R. G.; Barefield, E. K.; Hendrickson, D. N. *Inorg. Chem.* **1977**, *16*, 2746–2751. (b) Supp, R. C. *J. Chem. Phys.* **1959**, *30*, 326–327.
(18) Ringe, D.; Petsko, G. A.: Yamakura, F.; Suzuki, K.; Ohmori, D. *Proc. Natl. Acad. Sci. U.S.A.* **1983**, *80*, 3879–3883.
(19) Stallings, W. C.; Powers, T. B.; Pattridge, K. A.; Fee, J. A.; Ludwig, M. L., *Proc. Nat. Acad. Sci. USA* **1983**, *80*, 3884–3888.

Pagodane Dication, a Unique 2π-Aromatic Cyclobutanoid System[1]

G. K. Surya Prakash, V. V. Krishnamurthy, Rainer Herges, Robert Bau, Hanna Yuan, and George A. Olah*

Donald P. and Katherine B. Loker Hydrocarbon Research Institute and Department of Chemistry University of Southern California Los Angeles, California 90089-1661

Wolf-Dieter Fessner and Horst Prinzbach*

Chemisches Laboratorium der Universität Freiburg i. Br., Freiburg, West Germany

Received July 15, 1985

The highly symmetrical undecacyclic $C_{20}H_{20}$ hydrocarbon pagodone (**1**) (undecacyclo[9.9.0.0^{1,5}.0^{2,12}.0^{2,18}.0^{3,7}.0^{6,10}.0^{8,12}.0^{11,15}.0^{13,17}.0^{16,20}]eicosane) has been recently synthesized by Prinzbach et al.[2] as a potential precursor for its structurally related isomer dodecahedrane (**2**).[3] An isomerization pathway that can be considered would start with pagodane cations prepared under superacidic conditions. Previously we were successful[4] in isom-

(1) Considered Stable Carbocations. 267. University of Southern California. For part 266, see: Krishnamurthy, V. V.; Prakash, G. K. S.; Iyer, P. S.; Olah, G. A. *J. Am. Chem. Soc.*, in press.
(2) (a) Fessner, W.-D.; Prinzbach, H.; Rihs, G. *Tetrahedron Lett.* **1983**, 5857. (b) Fessner, W.-D. Dissertation, University of Freiburg, 1986. The dihydropagodane **7** (X = H) showed seven peaks in the ^{13}C NMR spectrum at δ ^{13}C 69.0 (singlet), 60.1 (doublet), 54.9 (doublet), 44.1 (doublet), 39.7 (doublet), 37.0 (triplet), and 34.7 (triplet).
(3) (a) Paquette, L. A.; Ternansky, R. J.; Balogh, D. W.; Kentgen, G. *J. Am. Chem. Soc.* **1983**, *105*, 5446.
(4) Olah, G. A.; Olah, J. A. *Synthesis* **1973**, 488.

0002-7863/86/1508-0836$01.50/0